Forest Ecology and Management 258 (2009) 1536–1548

Contents lists available at ScienceDirect

Forest Ecology and Management

journal homepage: www.elsevier.com/locate/foreco

Mapping dead wood distribution in a temperate hardwood forest using high resolution airborne imagery

Jon Pasher *, Douglas J. King

Geomatics and Landscape Ecology Laboratory, Department of Geography and Environmental Studies, Carleton University, 1125 Colonel By Drive, Ottawa, Ontario K1S 5B6, Canada

ARTICLE INFO

Article history:
Received 1 March 2009
Received in revised form 12 May 2009
Accepted 3 July 2009

Keywords:
Dead wood
Coarse woody debris
Snags
Remote sensing
Biodiversity indicator

ABSTRACT

Dead wood, in the form of coarse woody debris and standing dead wood, or snags, is an essential structural component of forest ecosystems. It plays a key role in nutrient cycling, ecosystem functions and provision of habitat for a wide variety of species. In order to manage dead wood in a temperate hardwood forest, an understanding of its availability and spatial distribution is important. This research evaluates airborne digital camera remote sensing for mapping temperate forest dead wood across an area within Gatineau Park, Canada. Two approaches were evaluated: (1) direct detection and mapping of canopy dead wood (dead branches and tall snags) through the combination of three techniques in a hybrid classification: ISODATA clustering, object-based classification, and spectral unmixing, and (2) indirect modelling of coarse woody debris and snags using spectral and spatial predictor variables extracted from the imagery. Indirect modelling did not provide useful results while direct detection was successful with field validation showing 94% accuracy for detected canopy level dead wood objects (i.e. 94% of validation sites with canopy dead wood were detected correctly) and 90% accuracy for control sites (i.e. 90% of validation sites with no canopy level dead wood were identified correctly). The procedures presented in this paper are repeatable and could be used to monitor dead wood over time, potentially contributing to applications in forest carbon budget estimation, biodiversity management, and forest inventory.

© 2009 Elsevier B.V. All rights reserved.

1. Introduction and background

The importance of dead wood in a forest is well understood as it plays an essential role in the health and functioning of the ecosystem at a variety of scales. Forest dead wood can be in the form of standing dead trees, commonly referred to as snags, as well as fallen material on the forest floor, referred to as woody debris, which is a direct result of dead or dying trees. Researchers and forest managers understand the benefits of dead wood in a forest in terms of its importance for nutrient cycling, long term carbon storage, as well as providing critical habitat for the maintenance of biodiversity (e.g. Stevens, 1997; McComb and Lindenmayer, 1999; Arsenault, 2002; Bull, 2002; Harmon, 2002; Tews et al., 2004; Tobin et al., 2007; Depro et al., 2008). Measures of dead wood are often incorporated in studies and protocols that monitor the health and biodiversity of forests, including national forest inventories (e.g. Canada's National Forest Inventory (CFIC, 2004)). As a result of the importance to forest ecosystems, dead wood has the potential to be used as an indicator of habitat or biodiversity on its own, as well as contributing to more comprehensive measures of overall structural complexity (e.g. McElhinny et al., 2006; Pasher and King, submitted for publication).

Snags can be inventoried through sampling (e.g. Bate et al., 1999; Kenning et al., 2005) and woody debris can be sampled using various methods (e.g. Van Wagner, 1964; Valentine et al., 2001; Stahl et al., 2002; Jordan et al., 2004). The non-uniform distribution of these structures in the forest (Ducey et al., 2002; Kenning et al., 2005) requires complex and intensive sampling strategies to properly survey an entire forest. Field methods are limited to point, line, or plot based sampling and, as a result, cannot provide spatially continuous information. Modern harvesting and forest management regulations often require a certain density or volume of dead wood to remain (following timber removal) in order to provide habitat and support ecosystem sustainability (e.g. Franklin et al., 1997; Holloway et al., 2007). Additionally, forest conservation in areas not managed for timber production is often concerned with identification of areas of high biodiversity potential. A continuous map showing the locations and spatial distribution of dead wood across a forest could support such management and conservation goals as well as be useful in habitat modelling and mapping for individual species.

* Corresponding author. Tel.: +1 613 520 2600x8439; fax: +1 613 520 4301.
E-mail address: jpasher@rogers.com (J. Pasher).

0378-1127/$ – see front matter © 2009 Elsevier B.V. All rights reserved.
doi:10.1016/j.foreco.2009.07.009

1.1. Research objectives

Based on the potential utility of spatially continuous information related to the distribution of dead wood across a forest, the goal of this research was to determine the potential of high resolution multispectral remote sensing for mapping dead wood across a temperate hardwood forest. The specific objectives were to: (1) evaluate *direct* detection using a hybrid classification process incorporating pixel, sub-pixel, and object-based information, (2) map the spatial distribution of dead wood across the forest, and (3) evaluate *indirect* regression-based modelling of downed and standing dead wood using spectral, spatial, and object-based image information.

1.2. Direct detection and mapping of dead wood

The direct detection and mapping of snags has shown potential in coniferous forests, as well as in deciduous forests specifically for the detection of dying oaks caused by sudden oak death. Butler and Schlaepfer, 2004 created snag distribution maps from 1:10 000 color infrared (CIR) air photos for spruce dominated forests within the sub-alpine zone in Switzerland. While the results were excellent, the research was carried out in sparse forests with isolated snags, and more importantly, it relied on manual photo interpretation and digitizing of dead trees, which is extremely time consuming. Others have used automated methods, including Haara and Nevalainen (2002) who developed a method to segment individual trees in 1:5000 CIR air photos of spruce dominated forests in southern Finland. For three forest stands, the average detection accuracy was 67% for dead and dying trees (61–100% needle loss). Leckie et al. (2004) used 60 cm resolution airborne multispectral imagery to detect and assess trees suffering from laminated root rot in Douglas fir forests in coastal British Columbia, Canada. They were able to successfully detect snags with fully intact crowns as well as those with missing branches using classification and automated tree crown delineation methods (Gougeon, 1995).

Several researchers have had success in mapping dead trees caused by sudden oak death in Californian hardwood forests. Kelly et al. (2004) evaluated three classification methods (unsupervised, supervised, and hybrid) applied to 1 m airborne multispectral imagery and achieved a best average accuracy of 96.3% using the hybrid classifier. Guo et al. (2007) developed a hybrid classification method combining object-based and knowledge-based classifications. It first segmented 1 m multispectral imagery into homogeneous objects and then used a set of rules to decide if each object was a dead crown (e.g. maximum size associated with known maximum crown size, compact shape, and adjacency to vegetation). Their results showed an accuracy of 96.1%, compared to supervised classification with an accuracy of 86.8%. Finally, Meentemeyer et al. (2008) were able to detect dead oak trees in 76% of sample field plots in the Big Sur ecoregion using an object-based classification and airborne color 33 cm pixel imagery.

1.3. Indirect modelling of dead wood

A variety of individual forest structural attributes such as stem density, diameter at breast height (DBH), basal area, crown diameter, canopy closure, leaf area index (LAI), etc. have been modelled using high resolution optical remote sensing spectral and spatial information (e.g. Wulder et al., 1998; Lévesque and King, 2003; Seed and King, 2003; Cosmopoulos and King, 2004), as well as other sensors, including airborne synthetic aperture radar (SAR) (Nelson et al., 2007) and laser/lidar data (Bater et al., 2007; Pesonen et al., 2008).

Remote sensing can potentially offer cost effective, rapid, and repeatable methods for inventorying dead wood across a forest. While woody debris for the most part would not be directly visible by airborne or satellite sensors, indirect modelling of coarse woody debris (CWD) can be conducted using image variables related to different aspects of forest structure that are manifested as image brightness variations. This is possible as a result of relationships that exist between dead wood and the surrounding forest structure, in particular the association of dead and dying trees with canopy gaps (Bursing, 2005; Kneeshaw and Prevost, 2007) or the presence of sparse tree crowns, which are visible in high resolution imagery.

In research carried out in Gatineau Park, Québec, Canada (the forest of this study) following a major ice storm in 1998, King et al. (2005) developed a model indirectly predicting the number of downed branches in fifteen field plots using spectral and spatial variables extracted from 25 cm resolution color infrared (CIR) photography (adjusted $R^2 = 0.71$, $p < 0.001$, standard error = 28.4% of observed mean (29.5 branches) in 20 m × 20 m plots. In a mixed boreal forest in Northern Ontario, Canada, Olthof and King (2000) developed a forest structure index (FSI) using canonical correlation analysis of linear relations between multiple image parameters and field-measured forest structural parameters. The index, which incorporated spectral, textural, and radiometric fraction image information extracted from 50 cm multispectral imagery, was used to explain the variance in a set of field variables that included measurements of fallen dead wood. Cosmopoulos and King (2004) refined the index methodology and applied it in temporal analysis of forest structural change. Working in old growth coniferous forests in Clayoquot Sound, British Columbia, Canada, more recently, Pesonen et al. (2008) used an airborne laser scanner (ALS) to model woody debris volume in thirty-three field plots in Finland (adjusted $R^2 = 0.61$, $p < 0.001$) based on two predictor variables representing the intensity of the last laser pulse and height variation extracted from the first pulse (i.e. top of canopy). While the model showed a strong R^2, it had an RMSE of 51.6% (14.09 m^3/ha).

Similarly, little research exists using remote sensing to indirectly model snags in the forest. Standing dead wood was also included as a structural variable in the forest structure index research of Olthof and King (2000) as described above. Bater et al. (2007) used a set of lidar variables in order to predict the percentage of dead trees within field plots. In order to overcome extremely skewed distributions, caused by the plots containing mostly live trees, they fit lognormal probability density functions to the frequency distributions of all the trees in the plots (including living and dead trees nine decay classes), and found the mean of the resultant distribution to be highly correlated with the percentage of dead trees ($r = 0.88$, $p < 0.001$). Their results showed good predictability of this parameter using different lidar variables, with R^2 ranging from 0.42 to 0.75. Pesonen et al. (2008) also modelled standing dead wood (snag) volume (adjusted $R^2 = 0.48$; RMSE = 78.8% (14.74 m^3/ha)) using the same ALS data mentioned above, leading to the conclusion that air photos were probably more suitable than laser scanning for indirect detection of standing dead trees.

2. Methods

2.1. Study area

This research was carried out in Gatineau Park, which extends from about 20 to 50 km Northwest of the city of Ottawa, Canada. More than 80% of the park's approximately 36 000 ha is forested, with approximately 55% dominated by hardwoods. The forest is dominated by sugar maple (*Acer saccharum* Marsh.), with small patches dominated by American beech (*Fagus grandifolia* Ehrh.), trembling aspen (*Populus tremuloides* Michx.), and red oak (*Quercus rubra* L.). Small numbers of red maple (*Acer rubrum* L.), American

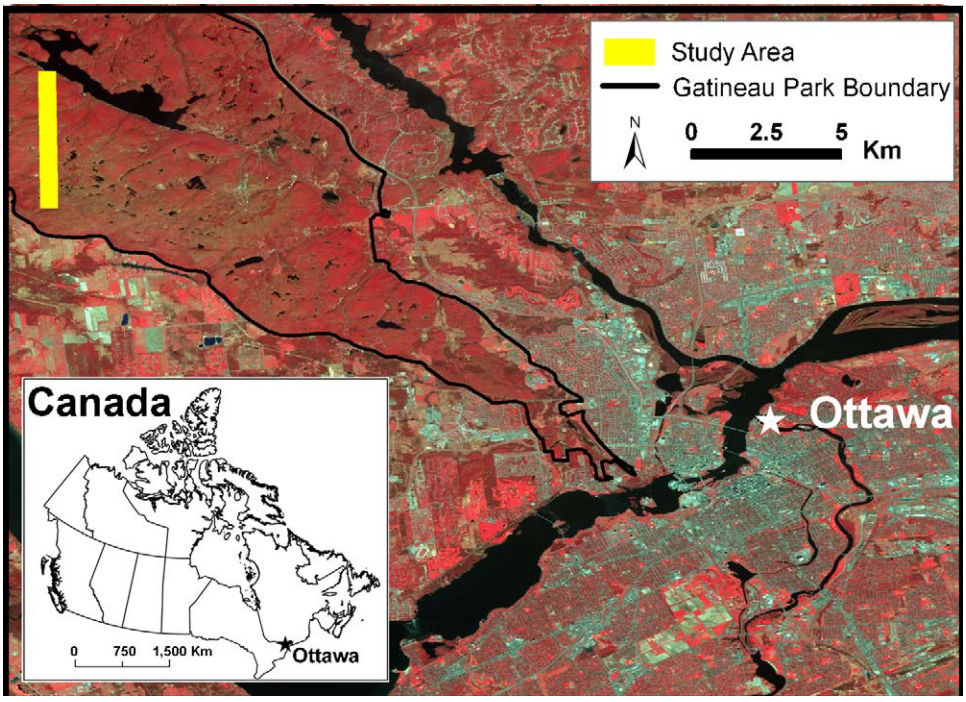

Fig. 1. Location of study area within the southern section of Gatineau Park near Ottawa, Canada (2005 SPOT satellite image in the background courtesy of P. Pellikka, University of Helsinki).

basswood (*Tilia americana* L.), ironwood (*Ostrya virginiana* (Mill.) K. Koch), white ash (*Fraxinus americana* L.), black ash (*Fraxinus nigra* Marsh.), white birch (*Betula papyrifera* Marsh.), and black cherry (*Prunus serotina* Ehrh.) are also present. Historical logging of white pine (*Pinus strobus*), which occurred in the area during the late nineteenth and early twentieth centuries, has greatly contributed to the forest's current composition (Lopoukhine, 1974; King et al., 2005; NCC, 2005).

The area of the forest used for this research (Fig. 1) corresponded to previous research that involved modelling and mapping ice storm damage in the park using remote sensing (King et al., 2005), as well as being used for other research associated with this paper involving modelling and mapping of forest structural complexity (Pasher and King, submitted for publication).

2.2. Initial field exploration

In order to better understand the types of snags present in the forest that should be detectable using the airborne imagery, along with any issues or potential problems that would be faced by this type of analysis, preliminary field excursions were conducted. It became evident that snags that were snapped off well below overstorey tree crowns would not be detectable but would be in shadows within the imagery. Snags with full or partial crowns intact, as well as snags without any branches that were close to the height of surrounding overstorey crowns, were considered to be potential targets (Fig. 2). It was obvious that CWD was not directly detectable, other than cases where large intact trunks lay beneath large gaps in the canopy, and therefore CWD was only investigated for potential indirect modelling purposes.

2.3. Remotely sensed imagery

Airborne imagery was acquired with 20 cm resolution using a Duncantech MS4100 CIR digital camera with a Nikon 24 mm lens. This high resolution imagery theoretically permitted snags or individual dead branches of approximately 20 cm in diameter to be detected given their reflectance differed significantly from surrounding foliage or shadow. The CIR imagery (green 500–600 nm, red 600–700 nm, near infrared 750–850 nm) was acquired over the study area on August 21st, 2007 at a flight altitude of 650 m. Individual images were corrected, in order to better represent actual surface reflectance, using a net correction procedure (Pasher and King, submitted for publication), which was used to remove brightness variations, typically found in airborne imagery, caused by sun-sensor-surface geometry (bi-directional reflectance variation (BRV), topographic variations, and lens effects (Teillet et al., 1982; Meyer et al., 1993; Pickup et al., 1995; Soenen et al., 2005)). The individual images, which each covered approximately 200 m × 200 m, were mosaiced together and georeferenced to two 2004, 25 cm orthophotos of Gatineau Park. Full details of imagery collection and processing can be found in Pasher and King (submitted for publication). The mosaic and georeferencing processes resulted in RMS errors of 2.56 m (X) and 2.29 m (Y), respectively.

2.4. Direct detection of dead wood in imagery

The multispectral imagery allowed clear manual identification of much of the dead wood in the upper canopy and some dead wood lower in the canopy or on the ground in large gaps. With respect to directly detecting dead wood in the imagery, the more general term "dead wood" will hereafter be used rather than snags, which was felt to be too specific and not representative of the objects that would possibly be detected. Although in some rare cases, CWD was thought to be detectable in the imagery, for the most part the objects that were investigated in this part of the analysis were snags, partially dead crowns and single dead branches within live crowns, all being indistinguishable from each other in the imagery. The partially dead crowns and single dead branches were deemed to indicate varying degrees of tree decline that would most likely produce CWD or snags within the next several years.

In the multispectral imagery, dead wood was visually distinguishable from surrounding live vegetation based mainly on its higher reflectance in the red band compared and its lower reflectance in the near-infrared (NIR) band (Jensen, 2006). For the

Fig. 2. Examples of snags thought to be suitable for detection and mapping, including those with fairly intact crowns (A and B) and those with no branches remaining (C and D), but found in canopy gaps and/or of heights similar to the surrounding live overstorey trees.

relatively small area of image coverage of this study, manual digitizing could have been used to delineate occurrences of dead wood and produce a map of its spatial distribution, however, the semi-automated methods investigated in this research could be applied more efficiently than manual interpretation for mapping much larger areas. As well, this research sought to investigate partially obscured dead wood within crowns and canopy shadows, which were not as easily identifiable. Three methods were used in combination in order to exploit different types of information in the spectral reflectance characteristics of dead wood compared to the surrounding foliage and shadows. Using the methods in combination was expected to increase the confidence in the detection of the individual objects.

2.4.1. ISODATA unsupervised clustering

Initially, an ISODATA unsupervised clustering algorithm was used as it is a common technique to automatically group pixels within an image into clusters using an iterative process based on the spectral properties of individual pixels (Jensen, 2006). Clustering techniques such as this were originally developed to be used at coarser scales for landcover mapping, but in this research it was used with high resolution imagery to create a thematic map of exposed wood isolated from the surrounding vegetation and from within crown shadows. This technique was used in a similar manner to Kelly et al. (2004) for creating a dead wood cluster. Twenty clusters were arbitrarily generated, and these were manually aggregated through comparison with the CIR imagery in order to produce a map of three classes representing exposed wood, live vegetation and canopy shadows. This map was then converted to a binary map representing the detected exposed wood (1) and everything else (0).

2.4.2. Sub-pixel wood fractions using linear spectral unmixing

As the ISODATA algorithm is a hard classifier, transition pixels between classes, for example pixels at edges between exposed wood and surrounding vegetation, are often confused as a result of their mixed radiance from more than one cover type. These pixels are assigned to one class based on a given rule such as the minimum distance of the pixel to each class mean (as in the ISODATA algorithm) or the probability of belonging to each class (as in the maximum likelihood classifier), however this can often result in a poor representation of reality (Settle and Drake, 1993; Oki et al., 2002). In addition, wood that is smaller than the pixel size and in shadow may not produce enough radiance to result in a hard classification as wood but may instead be assigned to the shadow class. As a result, soft classification techniques, such as linear spectral unmixing, have been developed that retain more information from within mixed pixels (Bastin, 1997). Since the reflectance of a pixel is often made up of more than one type of object, or scene component, spectral unmixing can be used to decompose the mixed spectra in order to determine sub-pixel proportions of each (Peddle et al., 2001). Given the "linear" nature of the procedure, the reflectance values associated with a mixed pixel are assumed to be linear combinations of the reflectance of the constituent classes that are within the bounds of that pixel (Klein Gebbinck, 1998; Brown, 2001). A constrained least squares linear unmixing procedure was used in order to produce images representing the fractional coverage of each class (Holben and Shimabukuro, 1993; Peddle et al., 2001).

Spectral unmixing relies on the selection of endmembers representing pure pixels of each of the desired classes to be used as training data. Endmember data were manually selected by delineating samples of the purest pixels of sunlit crowns (i.e. live vegetation), shadows, and exposed wood across the imagery (Pasher et al., 2007). Pixels were unmixed to created fractional coverages, including, of particular interest, a wood fraction image, similar to Lévesque and King (2003) and Pasher et al. (2007), with values for each pixel representing the fractional coverage ranging from 0 to 100% in terms of the wood content of that pixel. The wood fraction image was then converted to a binary image where all

pixels with wood fractions >50% (i.e. presumed to be made up of at least 50% wood) were classified as wood. This threshold was selected following visual interpretation and iterative testing of the effects of various thresholds on the resultant unmixed layer in order to best isolate those pixels that were in fact wood objects.

2.4.3. Object-based segmentation and classification

The final method used to isolate exposed wood within the imagery was a simplified object-based segmentation and classification method carried out using Definiens 5.0. This method works by segmenting, or partitioning, an image into multi-pixel objects, as opposed to an individual pixel based analysis (as for ISODATA clustering and spectral unmixing) in order to maximize between-object variance and minimize within-object variance (Flanders et al., 2003; Yan et al., 2006). Image segmentation was carried out based on visual assessments using the three segmentation parameters: scale, colour (spectral information), and shape (smoothness and compactness), which all contribute to the definition of objects and object sizes (Laliberte et al., 2004). The scale parameter is directly related to the resolution of the imagery and larger values result in larger objects (Benz et al., 2004). A value of 10 was eventually decided upon for this parameter. The colour parameter refers to the relative importance of an object's colour (reflectance) compared to its shape. For exposed wood in the imagery the reflectance was quite homogenous within the class, while the shapes were assumed to be quite heterogeneous. As well, the spectral differences between exposed wood and other objects (i.e. foliage and shadows) were extremely important and consistent as opposed to shape differences between classes, which may have varied significantly. Consequently, after iterative testing (Flanders et al., 2003; Yan et al., 2006), a ratio of 0.9:0.1 (colour:shape) was used. Given that the shape parameter was set to 0.1 (very low), the compactness/smoothness ratio did not have very much influence on the output objects and was therefore left at the default of 0.5:0.5, with tests showing little changes when these values were adjusted.

The resulting segmented objects were visually examined and found to closely resemble objects that would have been delineated through manual image interpretation. Following object segmentation, the objects were classified using a Nearest Neighbour classification (Definiens, 2006; Laliberte et al., 2006; Mallinis et al., 2008) based on spectral similarity to a sample of manually selected segmented wood objects that represented the variety of wood objects in the imagery. While fuzzy membership values, based on the Nearest Neighbour distance, were assigned to each object (Definiens, 2006), the classification was "hardened" by including all the objects that were assigned to the wood class. Objects with membership values greater than zero were assigned to a final classification layer, which resulted in a layer containing only those objects classified as wood across the imagery. While this selected membership value threshold could have impacted the actual number of detected objects in the classification, visual analysis of the segmented and classified objects showed a clear difference between wood objects and others in the imagery, a result of the reflectance characteristics of wood compared to foliage and shadows.

2.5. Developing a map of detected and delineated wood objects

The binary maps produced by the three dead wood detection methods were filtered to remove "salt-and-pepper" single pixel objects classified as wood, which were assumed to be erroneously detected objects, artifacts of the classification (similar to Guo et al., 2007), or very small parts of exposed wood, which were unfortunately impossible to validate in the field since individual wood objects of that size could not be identified within the canopy from the ground below. The layers were then generalized to remove the pixilated appearance and smooth the objects in order to provide more realistic areal estimates. Objects that were separated by a single pixel (i.e. only 20 cm apart) were combined by application of a single pixel buffer around each object. This had the effect of grouping multiple dead wood objects that were part of a single dead tree crown.

To produce a map with maximum confidence in terms of detected wood across the forest, the three layers were combined using a majority operation on a pixel by pixel basis. In other words, only those pixels that were classified as wood using at least two of the three methods were assigned to the wood class in the final map. While each method had its advantages and limitations in terms of utilization and results, the intersection of the three methods was thought to provide a much more robust and meaningful result. This approach is similar to the use of multiple, or hybrid classifiers (e.g. Steele, 2000; Kelly et al., 2004; Liu et al., 2004; Guo et al., 2007), which have shown increased accuracy over individual classifiers for detecting and mapping dead wood.

2.6. Field validation

Field validation of the map was carried out using sites that were completely independent of the creation of the map itself; any wood objects that were used as training data (e.g. for the unmixing endmembers and object-based classification) were not used in validation. To test the map accuracy in terms of its identification of the presence of dead wood, fifty dead wood objects were manually selected from the map for field validation. They were spatially distributed within three regions across the forest for accessibility and to be representative of the whole study area. They were also selected to represent the range of dead wood object sizes in the final map. In order to test the map's accuracy in terms of its representation of the absence of dead wood, and examine any errors of commission, a set of thirty sites (hereafter called control points) were selected in the forest, which according to the map showed no detected dead wood. Since there was some positional error caused by image georeferencing and the GPS, a 10 m radius buffer was used around each control point (i.e. a control point was selected if no dead wood was present on the map within 10 m).

The locations of all of the test wood objects ($n = 50$) and control points ($n = 30$) were randomized and loaded into a real time differential GPS that provided approximately 1 m horizontal accuracy. The identity of each point in terms of whether it was a delineated wood object or a control point was unknown to the researchers while they were in the field, with only a random identification number used to link the points to their known attributes that could be looked up following a visit to the field. This created a set of pseudo-independent and unbiased test points that were visited in the field without any *a priori* knowledge of whether the specific location in the field was mapped as a dead tree or with no significant wood object detected (i.e. control site).

Using the GPS the general location of each point was visited by researchers and small movements were made within the general vicinity of the locations in order to match the researchers' location with the location of the validation points on the GPS screen. This was done with the use of a 4 m external antenna, which ensured that enough satellites were used to maintain a stable signal with a low signal-to-noise ratio, providing submeter accuracy. Once the locations remained stable within a couple of meters for several minutes, the two researchers scanned the forest (in a radius of about 10 m to account for any image registration and GPS error) and recorded the presence or absence of any dead trees as well as other pertinent information about the surroundings that could potentially aid the interpretation of the results. While no specific size threshold was used to decide whether a dead tree was present,

any small dead trees (i.e. below the overstorey) that were found were examined and recorded to see if they were within a canopy gap and could therefore potentially be detected in the imagery.

2.7. Map of dead wood spatial distribution

A final map of the spatial distribution of dead wood across the forest was produced, similar to the methods presented by Meentemeyer et al. (2008), by calculating the total number of wood pixels found within a 400 m^2 area. This area was selected to match the size of study plots used in indirect modelling as explained in the following section.

2.8. Indirect regression modelling of dead wood

For regression based modelling of dead wood a plot-based approach was taken. In the summer of 2007 fifty 20 m × 20 m field plots were established across the study area in order to represent the range of structural and topographic conditions found across the forest. These plots were originally established for associated research by the authors investigating modelling and mapping forest structural complexity using high resolution remote sensing (Pasher and King, submitted for publication). Within the plots a variety of field measurements were taken based on the expected manifestation of structural conditions in the imagery, either directly (e.g. through crown sizes, canopy closure, or dead wood) or indirectly (e.g. the association of large CWD with overstorey gaps). Amongst these measurements, the number of snags in each plot was recorded, and volume of CWD was estimated (diameter >7.5 cm (Stevens, 1997; CFIC, 2004)) with the commonly used Van Wagner's (1964) method (e.g. Ter-Mikaelian et al., 2008):

$$V = \frac{\pi \sum d^2}{8L} \quad (1)$$

where V is the volume of CWD per unit area (m^3/ha), d is the diameter (cm) where it intersected the transect line, and L is the length (m) of the transect. Sampling was carried out along the diagonals of the plots, resulting in 56 m of transect length per plot.

Forward stepwise multiple regression was carried out in order to attempt to explain the variance of snag numbers and CWD volume, as well as the number of pieces observed. A variety of image predictor variables were input, including spectral, spatial, and object-based information (which had previously been untested for this application), as well as topographic information (elevation, slope, aspect) derived from a digital elevation model that had been previously derived photogrametrically from 25 cm pixel leaf-off orthophotos of the park. Variables such as the mean and standard deviation of spectral band brightness as well as the Normalized Difference Vegetation Index (NDVI) were calculated for each plot. As discussed earlier with regards to the direct detection of dead wood in the imagery, information extracted specifically from the red and NIR bands was expected to be representative of the presence and abundance of dead wood in the plots. Included in this group of image variables, the results from directly detecting dead wood using the hybrid classification approach presented previously in this paper were included as a potential predictor of field based dead wood.

Additionally, following the assumption that heterogeneity in the canopy caused by canopy gaps and the presence of dead wood would be detectable in the imagery, image spatial information was extracted from the imagery for each plot. Variables including textural measures derived from the gray-level co-occurrence matrix (Haralick et al., 1973), including Contrast, Entropy, ASM, Correlation, and Homogeneity, as well as the range and sill calculated from semivariograms for each spectral band, which have been shown to be useful for modelling various aspects of forest structure (Lévesque and King, 2003). Object-based variables including the number, size, and shape of delineated canopy objects were also included in the modelling as derived using a tree delineation algorithm (Pouliot et al., 2005). Complete details of these variables are given in Pasher and King (submitted for publication).

3. Results and discussion

3.1. Dead wood detection

Each of the three methods used to detect and delineate wood within the imagery produced slightly different maps. Fig. 3 shows an example of two large snags classified by the three methods to illustrate the delineations at the pixel level, with fully intact live tree crowns shown in comparison, along with visible shadows/canopy gaps. The generalization procedure that was carried out cleaned up the maps, and, as shown in an example of one of the three classification methods (Fig. 4), combined dead wood objects that were obviously part of the same snag, as well as removing the pixilated nature of the objects.

As expected, since it was the most basic method, the ISODATA clustering resulted in less than half of the area classified as wood compared to the other two methods (Table 1). The "hard" nature of the algorithm resulted in clusters that were composed solely of pure wood pixels. The transition, or mixed pixels between these wood objects and adjacent vegetation or shadow in the imagery were inconsistently classified and could not be easily associated with the pixels that were clearly wood. Even though the imagery was very high resolution (20 cm pixel size), small objects such as branches resulted in mixed pixels that were not well classified with the ISODATA algorithm. This result was also evident in the maximum size of wood objects, which, in the ISODATA map, was only 54.93 m^2, compared to 86.78 and 84.06 m^2 for the spectral unmixing and object-based methods, respectively.

The object-based segmentation produced a similar number of objects as unsupervised clustering (4 972 compared to 5 977). These two methods detected, in semi-automated fashion, only the most identifiable wood objects, very similar to those that would have been detected by manual image interpretation. On the other hand, the spectral unmixing method identified many smaller objects (resulting in approximately twice as many objects detected) within what appeared to be thick and healthy tree crowns as well as within dark shadow areas that were groups of very mixed pixels and potentially wood objects (Fig. 5).

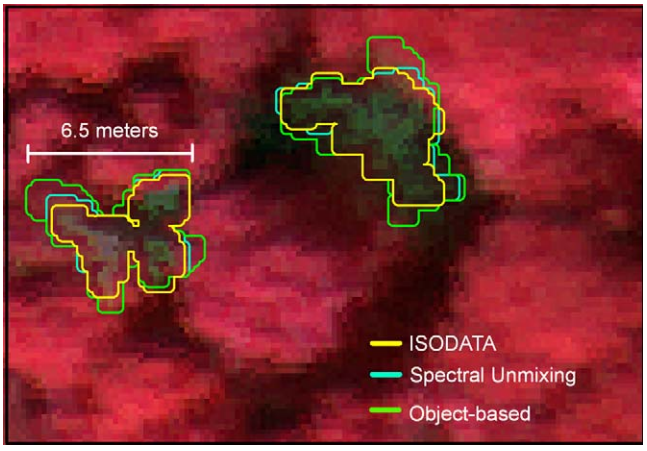

Fig. 3. A comparison of the three detection and delineation methods for two large snags shown with the CIR imagery in the background.

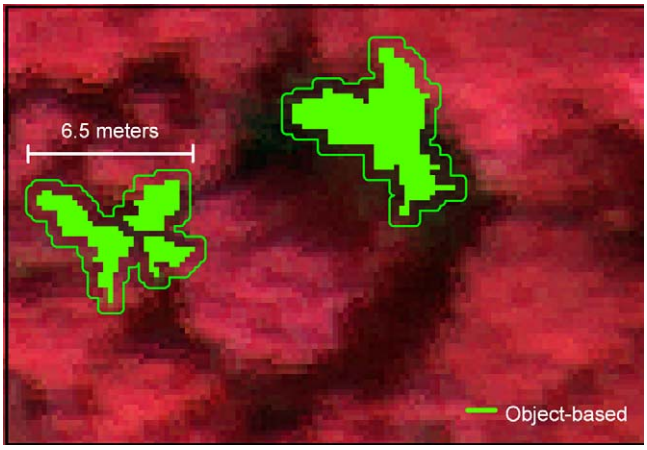

Fig. 4. An example of processing to group adjacent wood objects and generalize their boundaries. the object-based method is shown for illustrative purposes; the same method was also carried out for the other two classifications.

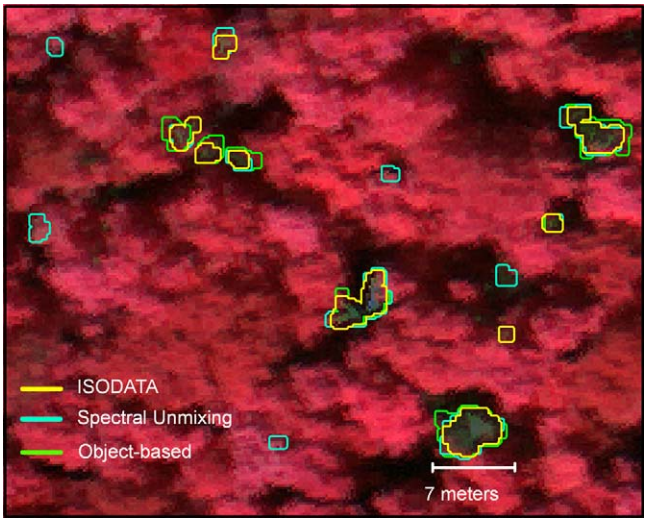

Fig. 5. A typical example of detected wood objects shown with the CIR imagery in the background. Spectral unmixing detected many small objects that were not detected by the other two methods.

The final map of wood objects, a result of the hybrid approach, contained only those objects with the highest probability of actually being wood objects in the forest, based on the assumption that if at least two of the three methods detected that object then the chance of it actually being a wood object in the forest and not a false positive was much higher (an example subarea is shown in Fig. 6). Based on this, many of the small objects previously discussed that were found by the unmixing method ended up being discarded, with the final map having only 6344 objects, ranging from 0.08 m^2 (only 1.5 pixels) to 82.52 m^2 (a dead crown of approximately 10 m diameter). While 96% of the objects detected using the ISODATA method and 88% of those detected using the object-based method matched in location (not necessarily in size) with the final objects, only 55% of the objects detected using spectral unmixing were included in the final classified map. Those objects not included in the final map (n = 5212) had areas ranging from 1.08 to 18.24 m^2 ($\bar{x}^2 = 2.06\,m^2$, S.D. = 1.24 m^2).

While unmixing detected approximately two times as many wood objects as the other two methods, most were very small and impossible to validate in the field. Increasing the fraction threshold to greater than 50% would reduce the number of wood objects detected, however, selection of a threshold is arbitrary. Testing of thresholds from 30% to 70% clearly showed an exponential decrease in the number of wood objects detected with increasing thresholds (r^2 of trendline = 0.99). The threshold of 50% was selected because of its ability to detect the significant and obvious wood objects based on tests done using manual interpretation. Thresholds smaller than 50% included too many objects that were interpreted as false positives, and too many pixels around the edges of known dead wood objects (examples shown in Fig. 7). As well, at thresholds less than 50% many single dead wood objects were represented by multiple image objects (examples shown in Fig. 7). Conversely, in many cases higher thresholds did not accurately capture the boundaries of obvious dead wood objects as a result of the mixed nature of the transition pixels. While maps created from unmixing may show more subtle detail than those produced from the per pixel methods it is doubtful that all the small wood objects detected represent significant habitat. As a result the unmixing method was in fact somewhat redundant for these purposes, with only 150 objects (out of 6344 objects) added to the final map that were not objects included as a result of a match between the ISODATA and object-based classifications. Given that this research had the goal of producing an accurate map of the relative dead wood spatial distribution across the forest, the dead crowns and large dead branches were of most interest, and not small dead branches within essentially healthy live crowns. These smaller objects may be useful for inventory purposes (e.g. for carbon modelling), however, from a validation point of view, without a close-up view of the top of the canopy (e.g. using a cherry-picker, ladder, or scaffolding (Barker and Pinard, 2001; Moorthy et al., 2007)), these objects would not have been visible on the ground beneath the canopy.

3.2. Map validation

Of the fifty detected wood objects that were used for validation, forty-one were correctly identified in the field as being snags, resulting in an accuracy of 82%. Of the 30 control point validation locations, where no wood object was found in the imagery, twenty-one were correctly identified in the forest, resulting in an accuracy of 70%. These control sites, which were selected to be at least 10 m away from a detected wood object in the imagery, were in fact on average 20.1 m (S.D. = 3.6 m) away from any wood object in the field, and therefore there should not have been any confusion regarding the location of the control site.

3.2.1. Assessment of errors of commission

While the results given above were thought to be successful overall, further investigation based on the field notes recorded at each of the eighty locations revealed interesting information that

Table 1
Wood object statistics as derived using the three different classification methods and by intersecting these three preliminary maps into a hybrid classification.

	N	Minimum (m^2)	Maximum (m^2)	Average (m^2)	Standard deviation (m^2)	Sum (m^2)
ISODATA clustering	4 972	1.12	54.93	3.47	3.70	17 250
Spectral unmixing	11 464	1.09	86.78	3.61	4.32	41 370
Object-based	5 977	1.36	84.06	6.16	6.29	36 818
Final hybrid map	6 344	0.08	82.52	4.41	4.98	27 969

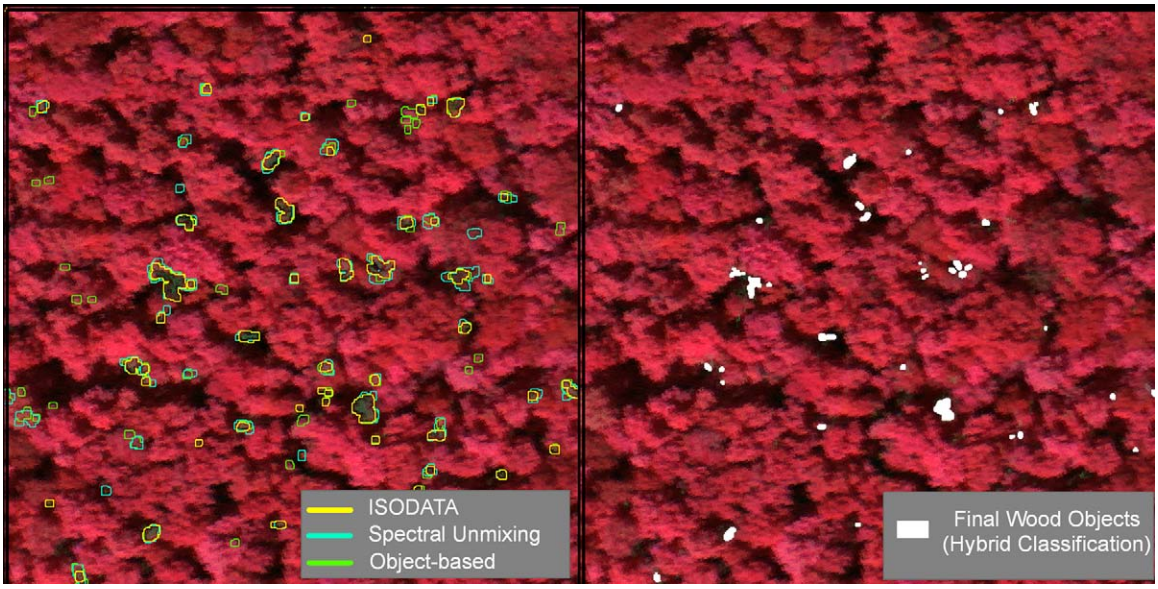

Fig. 6. A 100 m × 100 m section of the forest shown as an example of the detection/delineation by the three methods as well as the corresponding area of the final map of wood objects derived through the intersection of the three preliminary maps. Both images show the objects with the CIR imagery in the background.

aided explanation of the results and improved the mapping accuracies. Of the nine validation sites where a wood object was detected in the imagery but in the field this was found to be incorrect, two were described in the field notes as having a small dead crown in the vicinity that was not thought to be visible from the air. The surface areas of these dead trees, as measured in the imagery, were 2.95 and 4.14 m^2, which were close to the minimum size of the fifty validation wood objects (range of 1.37–27.10 m^2). These results suggest that some objects detected in the imagery were smaller than originally thought possible. Three additional sites initially assessed as incorrect had been noted in the field to have some dead branches and thin crowns in the canopy that were not expected to be detectable. However, these dead branches were probably more visible from above and detected in the imagery.

Given these explanations, the actual accuracy of the wood objects could in fact be increased from 82% to 92% (46 of 50 rather than 41 of 50), since at these five locations the dead wood that was detected in the imagery was actually found in the forest but it was smaller and less significant than originally thought possible for detection. The four remaining validation wood objects that were found to be incorrect had no significant dead wood in the vicinity. Three of these four errors, when examined in the imagery, were not obvious dead wood but appeared to be thin crowns that were not visible from the observer's position on the forest floor. Portions of branches in these crowns must have been exposed to the sensor view. The fourth location was actually one of the largest wood objects found, with an area of 21.96 m^2. Close examination of the imagery showed it to be above the surrounding overstorey canopy, and, as a result of shorter understorey trees, that are partially visible within a shadow in the imagery filling in the adjacent canopy gap (as seen in Fig. 8), this dead crown was not visible from the ground. In other words, the image detection procedure was correct while the field validation was incorrect, increasing the overall accuracy to 47 of 50, or 94%.

3.2.2. Assessment of errors of omission

When the erroneous control sites ($n = 9$), where a wood object was not detected in the imagery but one was found in the field, were examined in more detail, some interesting findings surfaced. Of these nine control sites, two had significant "pole" snags present, i.e., snags with no remaining intact crown or branches. This suggested that such snags were realistically not visible or detectable in the airborne imagery, most likely a result of camera view angles leaving the snag blocked from view by surrounding live crowns. Similarly, half-dead crowns were found at four of the other erroneous control sites, again seemingly a result of camera view angles. When examining the imagery more closely at these locations there was no sign of any dead wood that might have been missed by the algorithms. Thus, despite the narrow view angle (9.5° from nadir in all directions), some partially dead crowns were not visible to the sensor. These results demonstrate that no matter how well remote sensing algorithms work in detecting dead wood in imagery, the method should still only be used as a sampling, albeit a spatially continuous sampling, of the actual snags found in the forest, since many snags without any branches intact, as well as those snapped off below the overstorey, are not regularly detectable. In order to fully determine the proportion of dead wood detected in relation to that actually present, an intense survey of all of the dead trees in the forest would have to be conducted.

The remaining three erroneous control sites were truly errors of omission. These sites contained, as discovered and measured in the field, significant snags (two of them had dead crowns greater than 5 m in diameter as estimated from the ground) that were not detected in the imagery. These errors of omission were also potentially due to view angle and differential tree heights in the forest. This result suggests that potentially 10% of the forested area where no dead wood was detected could contain significant snags.

3.3. Mapping dead wood spatial distribution

The map of dead wood spatial distribution (Fig. 9) across the study area was patchy, reflecting the non-uniform distribution of dead trees that would be expected across a forest (Ducey et al., 2002; Kenning et al., 2005). The map was based on the number of detected wood pixels (each 20 cm × 20 cm) within a 400 m^2 area as calculated using a moving window passed across the image and therefore represented the relative distribution of dead wood across the forest.

The relative dead wood density was compared to the actual number of snags that had been counted in the field within the fifty field plots. A correlation of 0.53 ($p < 0.001$) was found, however the

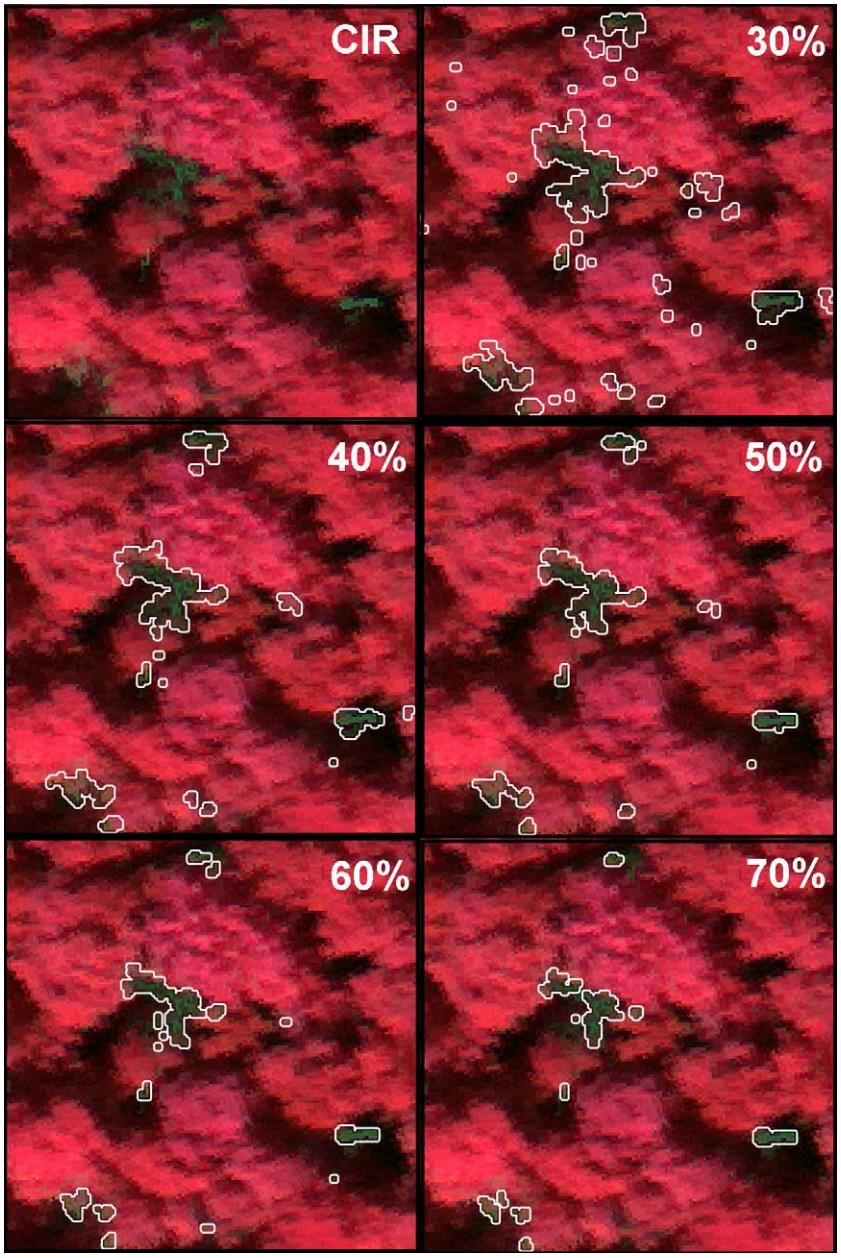

Fig. 7. Example 30 m × 30 m sample area showing results of testing to determine a suitable threshold for the 'hardening' of the unmixed fraction map. Dead wood object numbers and sizes vary with the thresholds shown (30–70%).

relationship was controlled by two field plots with a much greater number of snags (12 and 19) compared to an average of 4.88 (S.D. = 3.41) found in the fifty plots. While the relation was therefore not found to be a strong linear one and was in fact quite scattered, these findings suggest that this type of mapping could be used to identify areas in the forest with large numbers of snags (e.g. as in the lower left portion of Fig. 9). It must be noted that the plot estimates of snags included some snags below the canopy, which perhaps caused confusion within this relation.

The mapping method presented was able to produce a continuous and extensive map of the approximate distribution of dead wood across the study area. Compared to the time required to carry out field based sampling, processing imagery and producing a map from remotely sensed imagery is much faster. The acquisition of high resolution airborne imagery, such as was used for this analysis, can still be time consuming in terms of processing the individual images and creating a mosaic, however, commercially available automated acquisition and processing of digital aerial images would obviously greatly reduce this effort. While high resolution satellites do exist that could provide much greater coverage compared to an airborne imager (e.g. Quickbird imagery (~60 cm panchromatic and ~2.4 m multispectral (Digital Globe, 2008) or GeoEye-1 (~41 cm panchromatic and ~1.65 m multispectral (GeoEye, 2008)), the spatial resolution of the multispectral bands of these sensors is not considered to be appropriate for pixel level detection of dead wood in a temperate hardwood forest with the accuracy found in this study. Too much of the multispectral signal would be mixed and only the largest of snags would be detectable. However, spectral unmixing may improve on this and warrants further research.

One thing that must be kept in mind was that the dead trees detected in the study area, for the most part, were completely defoliated and quite small (average area = 4.41 m^2, ~1.18 m diameter using a circular approximation). The size of the dead

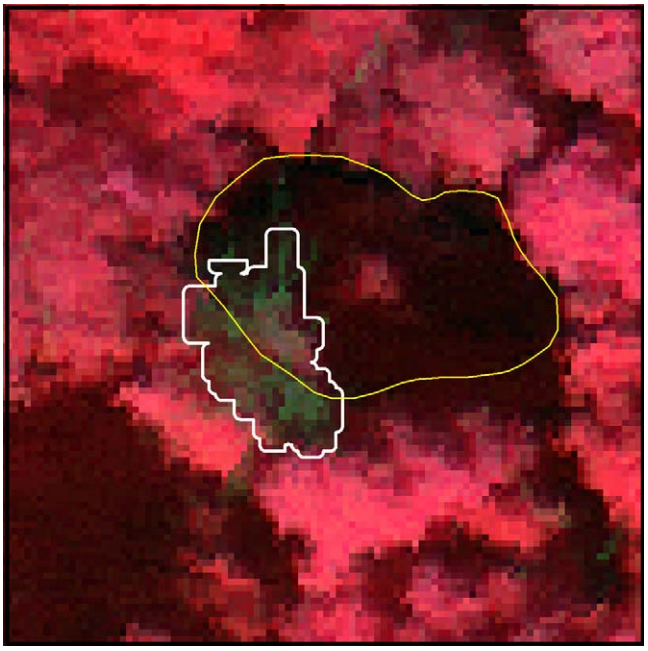

Fig. 8. A large dead wood object delineated in the imagery (white outline) that was not seen during field validation. The adjacent and overlapping area of the imagery that is outlined in yellow appears to be a live tree crown seen within a shadow in the canopy.

wood objects that were detected matched reasonably well with the measured crown diameters of 1056 live trees in the fifty field plots (Pasher and King, submitted for publication) which had an average crown diameter of 3.94 m^2 (S.D. = 1.28 m^2, min = 1.50 m^2, max = 14.30 m^2 (note that testing showed repeated crown diameter measurements to have a standard deviation of 0.70 m)). Similar research detecting dead trees in hardwood forests included that of Kelly et al. (2004), Guo et al. (2007), and Meentemeyer et al. (2008) who used imagery with resolutions of <1 m, ~1 m, and 33 cm, respectively, all carried out in Californian forests for detection of oak mortality caused by a pathogen. Statistics were not presented in their research with regard to the crown size of the mapped dead trees, so the relative success of these coarser resolution studies may have been due to larger trees

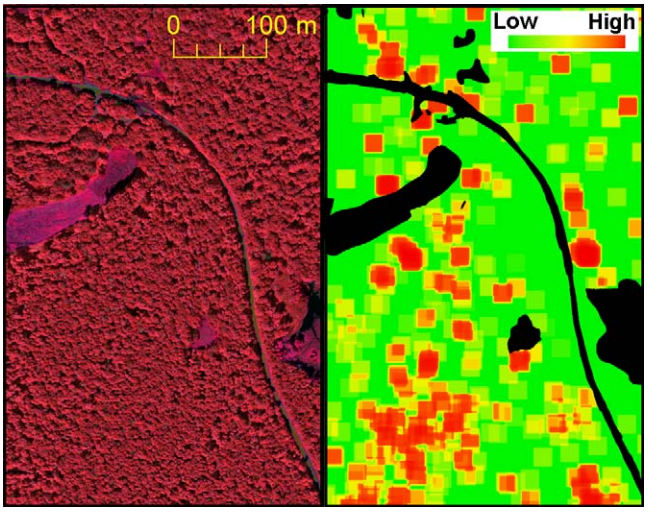

Fig. 9. An example subsection of the map of relative dead wood spatial distribution found across the forest as derived from the CIR imagery, shown for the corresponding area. Roads and water bodies were masked out and appear black on the map.

than those of this study or detection of foliage colour change typical of sudden oak death (Goheen, 2003). However, to detect smaller dead wood such as that shown in Fig. 2, higher resolution imagery is required.

The methods evaluated in this research could be used across any forest of interest, since the detection relied on the general spectral differences between exposed dead branches and the surrounding live vegetation, which to some degree exist in all forest types. Some study areas or types of forests may have large canopy gaps within which the bare ground is visible, requiring processing to differentiate between bare soil, litter or rock and dead wood when producing a map of detected wood objects (similarly to Kelly et al., 2004 and Guo et al., 2007).

3.4. Indirect modelling of dead wood

Field measurements in the fifty plots showed a range in the number of snags of 1–19 ($\bar{x} = 4.88$, S.D. = 3.41). The number of pieces of CWD ranged from 1 to 30 ($\bar{x} = 12.14$, S.D. = 6.86) and the volume of CWD ranged from 3.94 to 199.05 m^3/ha ($\bar{x} = 63.24\ m^3$/ha, S.D. = 47.05 m^3/ha), with the two found to be highly correlated ($r = 0.92$, $p < 0.001$). Unfortunately, the results from indirectly modelling plot based CWD and snags using variables extracted from the multispectral imagery were not as useful compared to the results presented from the direct mapping of canopy dead wood.

The best regression model for CWD volume (Table 2) was highly significant but only explained 30.3% of the variance and had a standard error of 39.27 m^3/ha, or 62.1% of the mean volume of all plots, compared to an RMSE of 28.4% found by King et al. (2005), albeit using the number of pieces rather than a measure of volume. The regression model derived in this case study for the number of pieces of CWD included similar variables but was not as strong as the one produced for CWD volume. Regression results were disappointing compared the study of King et al. (2005), which was carried out in the same forest. It is thought that the closeness of those measurements to the 1998 ice storm was potentially the reason for the successful indirect modelling of CWD using upper canopy spectral and spatial measures. Their plots represented a distinct gradient of damage from none to severe, the latter with large gaps, shadows and broken crowns (with associated CWD underneath) manifested as quite different image brightness and texture than in less damage plots. The plots for the research presented here were not specifically selected based on overstorey damage, and therefore it is possible that the same gradient found by King et al. (2005) did not exist to the same extent. As well, this research was carried out approximately 10 years following the storm, and while most of the CWD produced by the ice storm damage remained (Guo et al., 2006; Beets et al., 2008), the canopy had recovered relatively quickly (King and Bemrose, 2005). King et al.'s (2005) model included mean plot NIR brightness, the standard deviation of the NIR band, and mean plot red brightness as predictors of the number of downed branches. Similar variables were tested in the current research, but a poor relationship resulted due to the different canopy conditions.

The CWD volume model was difficult to interpret, however, the main predictor variable, which explained more than half of the variance, suggested that plots with fewer canopy objects had increasing amounts of CWD. The number of canopy objects, derived using a tree delineation algorithm (Pouliot et al., 2005), was significantly positively correlated with the number of overstorey trees ($r = 0.54$, $p < 0.001$). It is potentially indicative of plots that suffered from recent tree deaths, which contributed to the CWD that was found. However, the number of snags was not correlated with the CWD volume ($r = -0.05$, $p = 0.737$), which suggested there may have been a time lag since the trees died.

Table 2
Regression results for indirect modelling of coarse woody debris volume and the number of snags in fifty plots across the forest.

Dependent variable	R^2	Adjusted R^2	SE	Independent variables (contribution of variables shown by +/−)	Partial R^2	p
Coarse woody debris volume (m^3/ha)	0.346	0.303	39.27	− Number of canopy objects	0.213	<0.001
				− Variation of area of canopy objects	0.070	0.021
				+ Average NIR crowns	0.063	0.040
Number of snags	0.360	0.332	2.79	+ Total area wood	0.285	<0.001
				− Number of canopy objects	0.075	0.024

Interestingly, the third predictor variable included in the model showed increasing within crown NIR reflectance related to increasing amounts of CWD, supporting the idea that the CWD originated from historical fallen trees, and not partially damaged tree crowns, which would have exhibited lower average NIR reflectance.

The best model of the number of snags per plot explained slightly more variance (32.2%) (Table 2), however this model still had a very high error (SE = 2.79 or 57.2% of the mean number found in all plots). This model was more easily explained. It included only two predictor variables, with the first, the amount of dead wood found through classification (see Section 3.1), contributing 79% of the explained variance. The other variable included in the model was also object-based, as opposed to one reflecting spectral or spatial information in the imagery. The model showed that as the number of canopy objects found in the imagery decreased, the number of snags in the forest increased. This relationship was identical to the one shown in the regression model for CWD, however, similarly to the results previously discussed for CWD it was difficult to interpret since the number of snags in the plots was uncorrelated with the number of overstorey trees ($r = 0.10$, $p = 0.506$).

Relations between the number of snags and image predictor variables were poorer than expected. A contributing factor to this was clearly the fact that image variables were extracted over a 40 m^2 area, which corresponded to plot-based structural complexity research (Pasher and King, submitted for publication), and was also used to test indirect modelling in comparison to direct detection methods, which were carried out at a much finer scale. Image information extracted across the entire plot contained information from the vegetation and gaps that surrounded the snags, however snags made up such a small percentage of each plot in the imagery ($\bar{x} = 1.4\%$ and maximum was only 9.7%). As a result the information represented by the predictor variables potentially contained a large portion of noise, as opposed to information directly or indirectly associated with the snags. A smaller area could have been used for this research, possibly an area that corresponded with the size of crowns in the study area, however this would have resulted in an analysis almost identical to the direct detection methods that relied on local spectral and spatial information in the imagery.

4. Conclusions

This paper presents new research investigating the potential for semi-automated detection and mapping of dead wood within a temperate hardwood forest using airborne imagery. High resolution colour infrared airborne imagery was used along with various image processing methods in order to detect and delineate wood objects within the imagery. Validation showed detected dead wood objects to be accurately mapped (94%), while validation of sites mapped as non-dead wood had errors of about 10%. Indirect modelling of CWD and snags using spectral and spatial variables extracted from the imagery produce statistically significant models but their standard errors were 62 and 57%, respectively, leading to the conclusion that direct detection of canopy dead wood is better for spatially extensive mapping of the relative distribution of dead wood in a temperate hardwood forest. Further research using lidar data along with spectral and spatial variables extracted from airborne multispectral imagery might improve indirect modelling results, however the acquisition of lidar data over large areas is currently significantly more expensive compared to optical imagery.

While the direct detection methods are limited by sensor view angles and the 3-dimensional structure of a forest canopy, mapping results were promising for producing a spatially continuous representation of relative dead wood spatial distribution. This information has been used successfully as an input into forest structural complexity modelling and mapping in the context of habitat and biodiversity modelling, including in other research by the authors incorporating the information into an overall structural complexity index, along with a variety of other variables derived from the airborne imagery. This information could also be helpful for the management of habitat for individual or groups of species that rely on snags as keystone structures. As well, the methods and results could be used for improving forest management through the enhancement of forest inventories and possibly support research involving carbon budget modelling. Perhaps one of the most important points from this research is that the methods are highly automated and repeatable, and provide the ability to monitor changes over time of the presence and patterns of dead wood across a forest.

Acknowledgements

This research was funded by an NSERC Discovery grant to D. King. The Canada Foundation for Innovation, the Ontario Innovation Trust, the National Wildlife Research Centre and private sources funded Carleton University's Geomatics and Landscape Ecology Laboratory (GLEL), which provided all the necessary field equipment and data processing infrastructure used in this research. The authors are grateful to the NCC for access to Gatineau Park and for providing geospatial data used in this research. Many thanks to C. Czerwinski for his extensive help in the field, as well as M. Leni, V. Torontow, and R. Bemrose. The continuous feedback and advice of I. Olthof (Canada Centre for Remote Sensing), E. Humphreys (Geography, Carleton University) and J. Kerr (Biology, University of Ottawa) has been greatly appreciated.

References

Arsenault, A. 2002. Managing coarse woody debris in British Columbia's forests: a cultural shift for professional foresters. In: Proceedings of the Symposium on the Ecology and Management of Dead Wood in Western Forests, November 2–4, 1999; Reno, Nevada. Gen. Tech. Rep. PSW-GTR-181. U.S. Department of Agriculture, Forest Service, Pacific Southwest Research Station, Albany, CA, 949 pp.

Barker, M.G., Pinard, M.A., 2001. Forest canopy research: sampling problems and some solutions. Plant Ecology 153 (1-2), 23–38.

Bastin, L., 1997. Comparison of fuzzy c-means classification, linear mixture modelling and MLC probabilities as tools for unmixing coarse pixels. International Journal of Remote Sensing 18 (17), 3629–3648.

Bate, L J., Garton, E.O., Wisdom, M.J., 1999. Estimating snag and large tree densities and distributions on a landscape for wildlife management. Pacific Northwest Research Station; U.S. Department of Agriculture, Forest Service, Gen. Tech. Rep. PNW-GTR-425. Portland, OR, 76 pp.

Bater, C.W., Coops, N.C., Gergel, S.E., Goodwin, N.R., 2007. Towards the estimation of tree structural class in northwest coastal forests using Lidar remote sensing. In: P. Rönnholm, H. Hyyppä, J. Hyyppä (Eds.). Proceedings of ISPRS Workshop on Laser Scanning 2007 and SiliviLaser 2007, September 12–14, 2007, Finland. International Archives of Photogrammetry, Remote Sensing and Spatial Information Sciences XXXVI (Part 3/W52), pp. 38–43.

Beets, P.N., Hood, I.A., Kimberley, M.O., Oliver, G.R., Pearceand, S.H., Gardner, J.F., 2008. Coarse woody debris decay rates for seven indigenous tree species in the central North Island of New Zealand. Forest Ecology and Management 246 (4), 548–557.

Benz, U.C., Hofmann, P., Willhauck, G., Lingenfelder, I., Heynen, M., 2004. Multi-resolution, object-oriented fuzzy analysis of remote sensing data for GIS-ready information. ISPRS Journal of Photogrammetry & Remote Sensing 58, 239–258.

Brown, D.G., 2001. A spectral unmixing approach to leaf area index (LAI) estimation at the alpine treeline ecotone. In: Millington, A.C., Walsh, S.J., Osborne, P.E. (Eds.), GIS and Remote Sensing Applications in Biogeography and Ecology. Kluwer Academic Publishers, Boston.

Bull, E.L., 2002. The value of coarse woody debris to vertebrates in the Pacific Northwest. In: Proceedings of the Symposium on the Ecology and Management of Dead Wood in Western Forests, November 2–4, 1999; Reno, Nevada, Gen. Tech. Rep. PSW-GTR-181. U.S. Department of Agriculture, Forest Service, Pacific Southwest Research Station, Albany, CA, 949 pp.

Bursing, R.T., 2005. Tree mortality, canopy turnover, and woody detritus in old cover forests of the southern Appalachians. Ecology 86 (1), 73–84.

Butler, R., Schlaepfer, R., 2004. Spruce snag quantification by coupling colour infrared aerial photos and a GIS. Forest Ecology and Management 195 (3), 325–339.

Canadian Forest Inventory Committee (CFIC), 2004. Canada's National Forest Inventory—Ground sampling guidelines version 4.1, February 13th; 2004, 97 pp. https://nfi.nfis.org/documentation/ground_plot/Gp_guidelines_v4.1.pdf.

Cosmopoulos, P., King, D.J., 2004. Temporal analysis of forest structural condition at an acid mine site using multispectral digital camera imagery. International Journal of Remote Sensing 25 (12), 2259–2275.

Definiens, 2006. Definiens Professional 5 Reference Book. .

Depro, B.M., Murray, B.C., Alig, R.J., Shanks, A., 2008. Public land, timber harvests, and climate mitigation: quantifying carbon sequestration potential on U.S. public timberlands. Forest Ecology and Management 255, 1122–1134.

Ducey, M.J., Jordan, G.J., Gove, J.H., Valentine, H.T., 2002. A practical modification of horizontal line sampling for snag and cavity tree inventory. Canadian Journal of Forest Research 32 (7), 1217–1224.

Flanders, D., Hall-Beyer, M., Pereverzoff, J., 2003. Preliminary evaluation of eCognition object-based software for cut block delineation and feature extraction. Canadian Journal of Remote Sensing 29 (4), 441–452.

Franklin, J.F., Berg, D.R., Thornburgh, D.A., Tappeiner, J.C., 1997. Alternative silvicultural approaches to timber harvesting: variable retention harvest systems. In: Kohm, K.A., Franklin, J.F. (Eds.), Creating a Forestry for the 21st Century: The Science of Ecosystem Management. Island Press, Washington, DC, pp. 67–98.

Goheen, E.M., 2003. Detecting, surveying, and monitoring *Phytophthora ramorum* in forest ecosystems. In: Proceedings of the Sudden Oak Death Online Symposium. http://www.apsnet.org/online/SOD.

Gougeon, F.A., 1995. A crown-following approach to the automatic delineation of individual tree crowns in high spatial resolution aerial images. Canadian Journal of Remote Sensing 21 (3), 274–284.

Guo, L.B., Bek, E., Gifford, R.M., 2006. Woody debris in a 16-year old *Pinus radiata* plantation in Australia: mass, carbon and nitrogen stocks, and turnover. Forest Ecology and Management 228 (1–3), 145–151.

Guo, Q., Kelly, M., Gong, P., Liu, D., 2007. An object-based classification approach in mapping tree mortality using high spatial resolution imagery. GIScience & Remote Sensing 44 (1), 24–47.

Haara, A., Nevalainen, S., 2002. Detection of dead or defoliated spruces using digital aerial data. Forest Ecology and Management 160, 97–107.

Haralick, R.M., Shanmugan, K., Dinstein, I, 1973. Textural features for image classification. IEEE Transactions on Systems, Man, and Cybernetics 610–621 SMC-3.

Harmon, M.E., 2002. Moving towards a new paradigm for woody detritus management. USDA Forest Service General Technical Report PSW-GTR-181.

Holben, B.N., Shimabukuro, Y.E., 1993. Linear mixing model applied to coarse spatial resolution data from multispectral satellite sensors. International Journal of Remote Sensing 14 (11), 2231–2240.

Holloway, G.L., Caspersen, J.P., Vanderwel, M.C., Naylor, B.J., 2007. Cavity tree occurrence in hardwood forests of central Ontario. Forest Ecology and Management 239 (1–3), 191–199.

Jensen, J.R., 2006. Remote Sensing of the Environment: An Earth Resource Perspective, 2nd edition. Prentice Hall, Upper Saddle Hill, NJ, 592 pp.

Jordan, G.J., Ducey, M.J., Gove, J.H., 2004. Comparing line-intersect, fixed-area, and point relascope sampling for dead and downed coarse woody material in a managed northern hardwood forest. Canadian Journal of Forest Research 34 (8), 1766–1775.

Kelly, M., Shaari, D., Guo, Q., Liu, D., 2004. A comparison of standard and hybrid classifier methods for mapping hardwood mortality in areas affected by "sudden oak death". Photogrammetric Engineering & Remote Sensing 70 (11), 1229–1239.

Kenning, R.S., Ducey, M.J., Brissete, J.C., Gove, J.H., 2005. Field efficiency and bias of snag inventory methods. Canadian Journal of Forest Research 35 (12), 2900–2910.

King, D.J., Bemrose, R., 2005. Temporal analysis of field measured forest health response (1998–2004) following a severe ice storm. Contract report to the National Capital Commission, Ottawa, 14 pp. http://http-server.carleton.ca/~dking/papers/ncc05.pdf.

King, D.J., Olthof, I., Pellikka, P.K.E., Seed, E.D., Butson, C., 2005. Modelling and mapping forest ice storm damage using remote sensing and environmental data. Natural Hazards, Special Issue on Remote Sensing 35, 321–342.

Klein Gebbinck, M.S., 1998. Decomposition of mixed pixels in remote sensing images to improve the area estimation of agricultural field. PhD Thesis. Faculty of Mathematics and Informatics, University of Nijmegen, Jijmegen, The Netherlands.

Kneeshaw, D.D., Prevost, M., 2007. Natural canopy gap disturbances and their role in maintaining mixed-species forests of central Quebec, Canada. Canadian Journal of Forest Research 37 (9), 1534–1544.

Laliberte, A.S., Rango, A., Havstad, K.M., Paris, J.F., Beck, R.F., McNeely, R., Gonzalez, A.L., 2004. Object-oriented image analysis for mapping shrub encroachment from 1937 to 2003 in southern New Mexico. Remote Sensing of Environment 93 (1–2), 198–210.

Laliberte, A.S., Koppa, J., Fredrickson, E.L., Rango, A., 2006. Comparison of nearest neighbor and rule-based decision tree classification in an object-oriented environment. In: IEEE International Geoscience and Remote Sensing Symposium and 27th Canadian Symposium on Remote Sensing, July 31–August 4, Denver, CO.

Leckie, D.G., Jays, C., Gougeon, F.A., Sturrock, R.N., Paradine, D., 2004. Detection and assessment of trees with *Phellinus weirii* (laminated root rot) using high resolution multi-spectral imagery. International Journal of Remote Sensing 25 (4), 793–818.

Lévesque, J., King, D.J., 2003. Spatial analysis of radiometric fractions from high-resolution multispectral imagery for modelling individual tree crown and forest canopy structure and health. Remote Sensing of Environment 84, 589–602.

Liu, W., Gopal, S., Woodcock, C., 2004. Uncertainty and confidence in land cover classification using a hybrid classifier approach. Photogrammetric Engineering and Remote Sensing 70 (8), 963–971.

Lopoukhine, N., 1974. The forests and associated vegetation of Gatineau Park, Quebec. Forest Management Institute Information Report FMR-X-58, Study FM-72. Ottawa, Ontario.

Mallinis, G., Koutsias, N., Tsakiri-Strati, M., Karteris, M., 2008. Object-based classification using Quickbird imagery for delineating forest vegetation polygons in a Mediterranean test site. Journal of Photogrammetry and Remote Sensing 63, 237–250.

McComb, W., Lindenmayer, D., 1999. Dying, dead, and down trees. In: Hunter, M.L. (Ed.), Maintaining Biodiversity in Forest Ecosystems. Cambridge University Press, Cambridge, UK, p. 714.

McElhinny, C., Gibbons, P., Brack, C., 2006. An objective and quantitative methodology for constructing an index of stand structural complexity. Forest Ecology and Management 235, 54–71.

Meentemeyer, R.K., Rank, N.E., Shoemaker, D.A., Oneal, C.B., Wickland, A.C., Frangioso, K.M., Rizzo, D.M., 2008. Impact of sudden oak death on tree mortality in the Big Sur ecoregion of California. Biological Invasions 10 (8), 1243–1255.

Meyer, P., Itten, K.I., Kellenberger, T., Sandmeier, S., Sandmeier, R., 1993. Radiometric corrections of topographically induced effects on Landsat TM data in an alpine environment. Journal of Photogrammetry and Remote Sensing 48, 17–28.

Moorthy, I., Miller, J.R., Berni, J.A.J., Zarco-Tejada, P.J., Qingmou, L., 2007. Extracting tree crown properties from ground-based scanning laser data. In: Proceedings IEEE International Geoscience and Remote Sensing Symposium (IGARSS), Barcelona, Spain, pp. 2830–2832.

National Capital Commission (NCC), 2005. Gatineau Park Master Plan. http://www.ncc-ccn.gc.ca/data/2/rec_docs/1768_Master_Plan_e.pdf.

Nelson, R.F., Hyde, P., Johnson, P., Emessiene, B., Imhoff, M.L., Campbell, R., Edwards, W., 2007. Investigating Radar–Lidar synergy in a North Carolina pine forest. Remote Sensing of Environment 110 (1), 98–108.

Oki, K., Oguma, H., Sugita, M., 2002. Sub-pixel classification of alder trees using multitemporal Landsat Thematic Mapper imagery. Photogrammetric Engineering and Remote Sensing 68 (1), 77–82.

Olthof, I., King, D.J., 2000. Development of a forest health index using multispectral airborne digital camera imagery. Canadian Journal of Remote Sensing 26, 166–176.

Pasher, J., King, D.J., Lindsay, K., 2007. Modelling and mapping potential hooded warbler (*Wilsonia citrina*) habitat using remotely sensed imagery. Remote Sensing of Environment 107 (3), 471–483.

Peddle, D.R., Brunke, S.P., Hall, F.G., 2001. A comparison of spectral mixture analysis and ten vegetation indices for estimating boreal forest biophysical information from airborne data. Canadian Journal of Remote Sensing 27 (6), 627–635.

Pesonen, A., Maltamo, M., Eerikainen, K., Packalen, P., 2008. Airborne laser scanning-based prediction of coarse woody debris volumes in a conservation area. Forest Ecology and Management 255 (3288), 3296.

Pickup, G., Chewings, V.H., Pearce, G., 1995. Procedures for correcting high resolution airborne video imagery. International Journal of Remote Sensing 16, 1647–1662.

Pouliot, D.A., King, D.J., Pitt, D.G., 2005. Development and evaluation of an automated tree detection-delineation algorithm for monitoring regenerating coniferous forests. Canadian Journal of Forest Research 35, 2332–2345.

Seed, E.D., King, D.J., 2003. Shadow brightness and shadow fraction relations with effective LAI: importance of canopy closure and view angle in mixedwood boreal forest. Canadian Journal of Remote Sensing 29 (3), 324–335 Special issue on measurement and use of leaf area index in monitoring vegetated ecosystems.

Settle, J.J., Drake, N.A., 1993. Linear mixing and the estimation of ground cover proportions. International Journal of Remote Sensing 14 (6), 1159–1177.

Soenen, S.A., Peddle, D.R., Coburn, C.A., 2005. SCS+C: a modified sun-canopy-sensor topographic correction in forested terrain. IEEE Transactions on Geoscience and Remote Sensing 43, 2148–2159.

Stahl, G., Ringvall, A., Gove, J.H., Ducey, M.J., 2002. Correction for slope in point and transect relascope sampling of downed coarse woody debris. Forest Science 48 (1), 85–92.

Steele, B.M., 2000. Combining multiple classifiers: an application using spatial and remotely sensed information for land cover type mapping. Remote Sensing of Environment 74 (3), 545–556.

Stevens, V., 1997. The ecological role of coarse woody debris: an overview of the ecological importance of CWD in B.C. forests. Research Branch, British Columbia Ministry of Forestry. Victorial, B.C. Working Paper 30/1997.

Teillet, P.M., Guindon, B., Goodenough, D.G., 1982. On the slope-aspect correction of multispectral scanner data. Canadian Journal of Remote Sensing 8, 84–106.

Ter-Mikaelian, M.T., Colombo, S.J., Chen, J.X., 2008. Amount of downed woody debris and its prediction using stand characteristics in boreal and mixedwood forests of Ontario, Canada. Canadian Journal of Forest Research 38 (8), 2189–2197.

Tews, J., Brose, U., Grimm, V., Tielborger, K., Wichmann, M.C., Schwager, M., Jeltsch, F., 2004. Animal species diversity driven by habitat heterogeneity/diversity: the importance of keystone structures. Journal of Biogeography 31, 79–92.

Tobin, B., Black, K., McGurdy, L., Nieuwenhuis, M., 2007. Estimates of decay rates of components of course woody debris in thinned Sitka spruce forests. Forestry 80 (4), 455–469.

Valentine, H.T., Gove, J.H., Gregoire, T.G., 2001. Monte Carlo approach to sampling forested tracts with lines or points. Canadian Journal of Forest Research 31 (8:), 1410–1424.Grey, A.N., Azuma, D.L., 2001. Repeatability and implementation of a forest vegetation indicator. Ecological Indicators 5 (1), 57–71.

Van Wagner, C.E., 1964. The line intersect method in forest fuel sampling. Forest Science 14 (1), 20–26.

Wulder, M.A., LeDrew, E.F., Franklin, S.E., Lavigne, M.B., 1998. Aerial image texture information in the estimation of northern deciduous and mixed wood forest leaf area index (LAI). Remote Sensing of Environment 64 (1), 64–76.Zenner, E.K., 1998. Do residual trees increase structural complexity in Pacific Northwest coniferous forests? Ecological Applications 10 (3), 800–810.

Yan, G., Mas, J.F., Maathius, B.H.P., Xiangmin, Z., Van Dijk, P.M., 2006. Comparison of pixel-based and object-oriented image classification approaches—a case study in a coal fire area, Wuda, Inner Mongolia, China. International Journal of Remote Sensing 27 (18), 4039–4055.